nature materials

Perspective

https://doi.org/10.1038/s41563-024-01814-2

Creating chirality in the nearly two dimensions

Received: 18 May 2023

Accepted: 18 January 2024

Published online: 22 February 2024

Check for updates

Hanyu Zhu [1] & Boris I. Yakobson [1,2]

Structural chirality, defined as the lack of mirror symmetry in materials' atomic structure, is only meaningful in three-dimensional space. Yet two-dimensional (2D) materials, despite their small thickness, can show chirality that enables prominent asymmetric optical, electrical and magnetic properties. In this Perspective, we first discuss the possible definition and mathematical description of '2D chiral materials', and the intriguing physics enabled by structural chirality in van der Waals 2D homobilayers and heterostructures, such as circular dichroism, chiral plasmons and the nonlinear Hall effect. We then summarize the recent experimental progress and approaches to induce and control structural chirality in 2D materials from monolayers to superlattices. Finally, we postulate a few unique opportunities offered by 2D chiral materials, the synthesis and new properties of which can potentially lead to chiral optoelectronic devices and possibly materials for enantioselective photochemistry.

Nature is inherently chiral. From the molecular biology of all organisms to the laws of particle physics, the concept of chirality and the spontaneous breaking of symmetry have fascinated generations of scientists. The exact symmetry (or symmetries) broken by chirality, however, can differ remarkably across the disciplines. Here we refer to the oldest and arguably the most common notion of 'chiral' materials, that is, the lack of mirror symmetry, meaning that after mirroring a chiral object, we cannot completely overlap it with the original object by any translation and/or rotation. The structural chirality is not equivalent to the breaking of inversion, time-reversal and/or particle–hole symmetries that are often invoked in various fields of physics[1,2]. The manifestation of chiral properties is closely connected with spatial dimensionality: a strictly flat object with no mirror lines (as letters 'b' and 'd') may seem chiral if its moves are restricted to the two-dimensional (2D) space, but it is nevertheless not chiral for all relevant physical observations that occur in three-dimensional (3D) space, where the object itself serves as a mirror plane. Then the question is, how one can talk about chirality in 2D materials? Of course, there is no 'truly 2D' material, as every atom and bond has finite volume, but interesting science occurs when the minute 3D structural chirality at the atomic scale creates disproportionally large and useful effects, while still leveraging unique 2D physics such as strong Coulomb interactions, topological singularities, and externally tunable electronic and magnetic parameters[3–5].

Since the discovery of optical circular birefringence in quartz in the early 1800s[6], chiral photonic and chemical properties have been extensively studied in crystals, molecules, and micro- and nanostructures. Chiral materials, for example, have recently been utilized for optoelectronic and spintronic functionalities ranging from helicity-dependent beam-splitting[7], second-order optical nonlinearity[8], chiral-induced spin selectivity (CISS)[9] and topological transport[10]. There are many routes to make chiral crystals. Naturally, chiral molecules may crystallize into chiral crystals or facilitate the formation of chiral structures. More intriguingly, non-chiral building units can also form chiral crystals that constitute a substantial fraction of chiral materials[11]. Thus, although only a handful of 2D van der Waals (vdW) layered materials are intrinsically chiral[12], the nearly unlimited possibility of warping and assembly suggests a prolific platform to control and enhance chiral phenomena[13].

Borrowing the concepts developed by the large volume of existing literature on chiral molecules and nearly one-dimensional (1D) materials, one can start with systematically examining the ways to construct chirality from identical 2D unit cells. First, a molecular unit possessing some chirality *c*, such as the chiral centre in Fig. 1a, will always form a chiral material regardless of the lattice geometry. Next, achiral units can also arrange into chiral structures. Consider if the units repeat along a 1D curve in 3D Euclidean space, the resulting structure corresponds

[1]Department of Materials Science and NanoEngineering, Rice University, Houston, TX, USA. [2]Department of Chemistry, Rice University, Houston, TX, USA. e-mail: hanyu.zhu@rice.edu; biy@rice.edu

https://doi.org/10.1038/s41563-024-01814-2

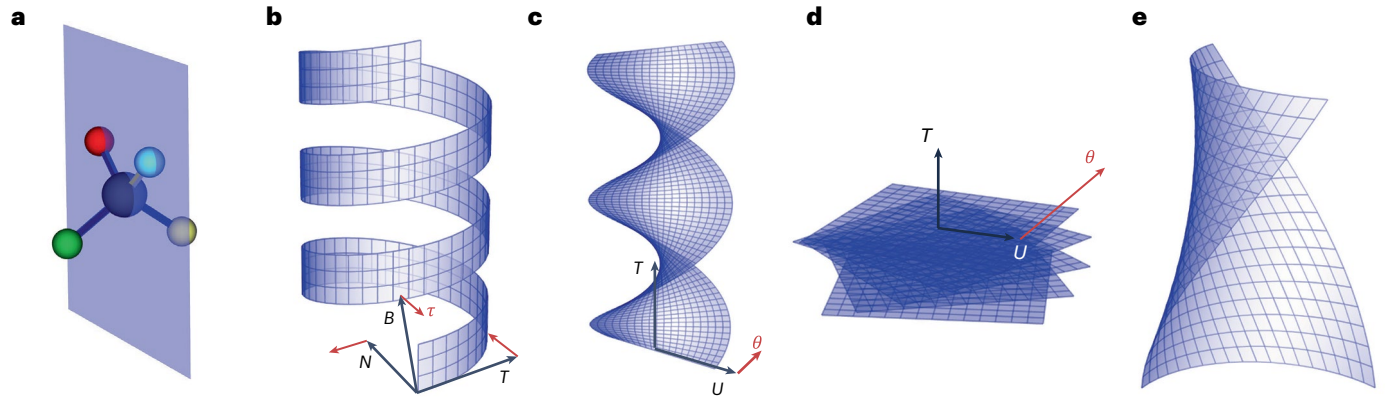

Fig. 1 | Types of chiral nearly 2D materials. a, A flat lattice with chiral unit cells. **b**, Non-chiral unit cells in a helical ribbon lattice with pure torsion τ. Black arrows represent: T, the unit tangent vector of the helix; N, the unit normal vector; and B, the unit binormal vector. Red arrows indicate the rates of rotation of the corresponding vectors along the curve. **c**, A ribbon with the unit vector U and pure twist θ around the tangent to the curve. U denotes the unit ribbon vector. **d**, A twisted few-layer stack of flat 2D planes. **e**, A general chiral plane with non-zero torsion, twist and finite curvature.

to the concept of ribbon in differential geometry. A periodic curve with a constant curvature and a constant torsion τ, defined as the rate of rotation of the unit binormal vector, is a helix. The ribbon additionally has an intrinsic twist θ, defined as the rate of rotation of the unit ribbon vector around the curve. These two parameters are, in theory, all that are needed to define nearly 1D periodic chiral structures[14]. The handedness of the ribbon can be defined by the sign of the 'total twist' $\tau + \theta$. It might be heuristically appealing to construct the total chirality by including the structure of the molecular unit, as '$c + \tau + \theta$'; however, c can neither be parameterized nor be given a sign[15]. The total twist is usually a good indicator of the sign and the strength of local chiral effects, even if strictly speaking, local twist may not fully determine the global chirality of a structure.

Now concerning nearly 2D or 3D periodic structures, if there is no or only one non-zero principal curvature, the structures will be a trivial extension of the 1D cases discussed above. Depending on the shape of the units as well as the magnitude of τ and θ, the resulting materials may have vastly different appearance. For example, a 2D film with in-plane shear and out-of-plane curvature, as shown in Fig. 1b, resembles a nearly 1D carbon nanotube[16]. A 2D film twisting around an in-plane curve is a helicoid (Fig. 1c), which was theoretically proposed and experimentally demonstrated with graphene[17,18]. The twisting axis can be out-of-plane as well for a nearly 2D stacking, like in Fig. 1d. A general structure should be regarded as chiral (Fig. 1e), as long as the total twist is non-zero at any point. Then, considering non-Euclidean structures with more than one non-zero principal curvatures embedded in 3D space, the material shall either be spatially non-uniform or contain topological defects, for example, disclinations in the lattice of units. That is to say, spatially uniform chiral crystals are always geometrically linked to nearly 1D chiral structures, so they share many properties that have been extensively studied theoretically and experimentally. Nevertheless, chiral nearly 2D materials may have quantitatively superior performance and some technological advantages in large-scale fabrication, and thus deserve more systematic investigations[13,19].

Emergent chiral properties in vdW 2D bilayers

For materials made by stacking 2D vdW layers, the twist of the stack nearly always yields chirality, unless the interlayer angle is $360°/2n$ for n-fold symmetric layers. So far, the exploration of twisted homobilayers and heterostructures, coined 'twistronics', has mainly focused on the tunable periodic potentials of the produced moiré superlattices, but not the chirality per se[20,21]. The moiré potential alters the band structure to enhance Van Hove singularity and effective interaction strength, both of which are scalars unaffected by the handedness of the structure. Meanwhile, the twist-induced chirality has not been entirely overlooked. For example, twisted bilayer graphene exhibits giant circular dichroism (CD) two orders of magnitude larger than typical organic molecules, when normalized by mass per area[22], as shown in Fig. 2a–c. The enhancement is attributed to the large optical conductivity in the atomic layers and a large interlayer transition. Chiral optical resonances are also expected from inter-miniband transitions of near-magic-angle twisted bilayer graphene[23]. Interestingly, CD means that the material receives a net circularly polarized excitation from the incident non-polarized infrared light. Such excitation can first convert to a valley-polarized plasmon through the valley-dependent optical selection rules, meaning that the distribution of electron–hole pairs is asymmetric in the momentum space, which breaks time-reversal symmetry (TRS). In parallel, the broken inversion symmetry from chirality also ensures finite valley-contrasting Berry curvature, although strictly speaking, structural chirality is not required for finite Berry curvature. Thus, the valley polarization can then induce a Hall-like net transverse conductivity as though the material is under a strong magnetic field up to 10 T, leading to unidirectionally rotating 'chiral' plasmon modes in the sense of TRS breaking[24], shown in Fig. 2d,e. The net effect of these two steps is an elegant example of how the structural chirality plus a finite momentum (in this case from the incident light) is 'similar' in terms of symmetry operations to a rotating in-plane field[25], which is sometimes also called 'chiral' in 2 + 1D space. In another study, the chirality of twisted bilayer graphene was theoretically found to enable localized edge plasmons, whose dispersion resembles that of the magnetoplasmon in monolayer graphene created by a large out-of-plane magnetic field, despite that the symmetries of the plasmon eigenmodes are different[26].

Similar to the high-frequency chiral optical response, a low-frequency transport phenomenon called the nonlinear Hall effect (NHE) exists in twisted graphene and transition-metal dichalcogenide (WSe_2) bilayers, as well as graphene/hexagonal boron nitride heterostructures[27–30]: the broken mirror symmetry from structural chirality enables a Berry curvature dipole, which is originally forbidden by the C_{3v} symmetry[31]. The chirality-induced Berry curvature dipole differs from another NHE mechanism that requires only inversion-symmetry breaking, the skew scattering, where an external electric field excites valley-polarized electrons due to the trigonal wrapping of the band structure, resulting in valley Hall conductivity. For both mechanisms, the Hall voltage is proportional to the square of the longitudinal electric field (Fig. 2f), but the relative contribution from the two mechanisms varies greatly among materials. In WSe_2, although inversion symmetry is already broken in individual monolayers, the chirality of the twisted bilayer enhances the NHE by several orders of magnitude[27]. But in graphene/hexagonal boron nitride heterostructures, the NHE from the Berry curvature dipole, caused by either uniaxial strain or chirality,

https://doi.org/10.1038/s41563-024-01814-2

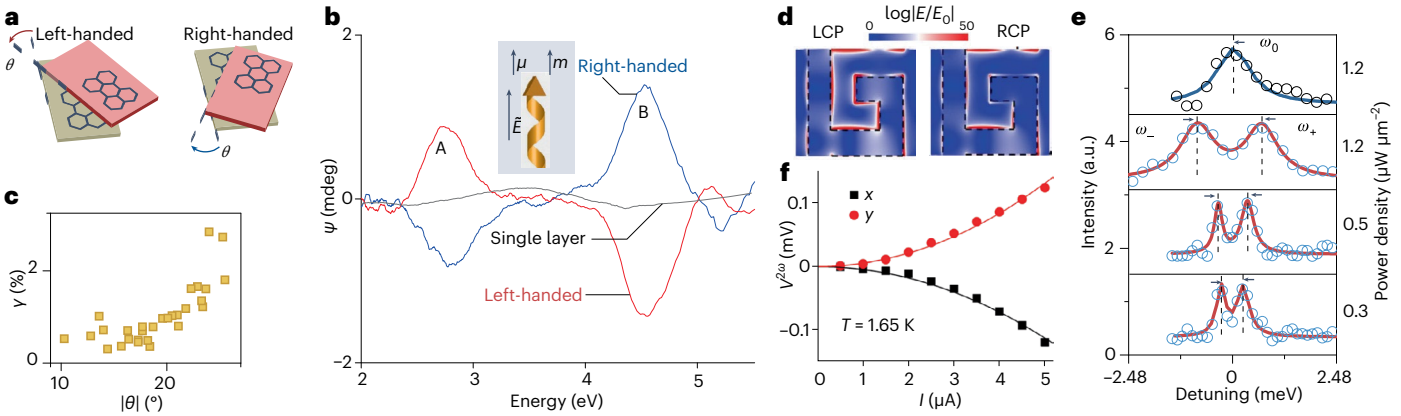

Fig. 2 | Experimental observations of chiral scattering and transport properties in twisted bilayer graphene at optical, infrared and zero frequencies. a,**b**, The positive and negative twisting angles result in opposite structural handedness (**a**), as well as opposite optical ellipticity ψ (**b**), as a result of co-existing electric (μ) and magnetic (m) dipoles induced by an oscillating electric field $\bar{E}$ in a chiral material (inset). A and B denote two interlayer optical resonances tunable by the twisting angle. **c**, The chiral interlayer transition γ grows as a function of twisting angle θ. **d**, Infrared circular dichroism leads to valley polarization and a 'chiral' plasmon, which then differentiates the left-circular polarized (LCP) and right-circular polarized (RCP) plasmonic modes in a spiral resonator, which are visualized by the simulated spatial distribution of the enhanced electric field (E) with respect to the incident electric field (E_0). **e**, Compared with a straight nanoribbon whose resonance is centred around ω_0 = 76 meV (blue curve, shifted to zero detuning), the spiral resonator shows two modes ω_- and ω_+, whose splitting (black arrows) is proportional to the intensity of the incident light. Open circles, measured spectra; solid curves, Lorentzian fitting; dashed lines, peak position. **f**, A longitudinal current I induces valley polarization, as well as nonlinear longitudinal (x) and transverse Hall (y) voltage $V^{2\omega}$. T, temperature. Panels adapted with permission from: **a**–**c**, ref. 22, Springer Nature Ltd; **d**,**e**, ref. 24, Springer Nature Ltd. Panel **f** reproduced with permission from ref. 29, Springer Nature Ltd.

becomes dominant only in the clean limit with low disorder density[30]. In all the cases above, it is important to note that chiral optical or electronic properties are only possible without the particle–hole symmetry, which holds approximately near a Dirac point but breaks if the Fermi level is tuned away from the charge-neutral point[32,33].

Last but not least, magnetic 2D materials spontaneously break TRS, and if made structurally chiral, allow asymmetric spin exchange interactions, leading to interesting non-collinear and topological spin textures[34,35]. Again, it is possible to create driven spin polarization in initially non-magnetic twisted bilayers by breaking TRS with external current, and then the chiral interactions among the spins may result in unconventional magnetism[36]. Apart from these emerging properties reported in experiments and calculations, chiral vdW materials have also been shown to host strong chiral-induced spin selectivity and topological Kramers–Weyl fermions[37,38], which are potential platforms for robust spin transport properties[39].

The magnitude of chiral effects in twisted 2D materials, intuitively, should be determined by the relative strength of the interlayer coupling such as mechanical forces, electronic hopping and spin exchange interaction across the vdW interface with respect to the intralayer coupling. Here we limit our discussion to microscopic phenomena arising from the asymmetry of electronic and atomic wavefunctions, such as band structures, and will not elaborate on long-range electromagnetic interactions in macroscopic chiral structures, such as solenoids or chiral photonics. The microscopic asymmetry could be the key to justifying '2D chiral materials', by comparing the thickness of the materials with other relevant length scales, such as the lateral size or the coherent length of an electronic device, the effective wavelength of light in the materials and so on. Optical CD is a great example to examine the definition of 'two-dimensionality', because strictly speaking, CD is a 3D phenomenon whose magnitude is usually proportional to the 'asymmetry in the third dimension' of a structure. Indeed, in twisted bilayers, CD contains a pre-factor of thickness, and thus becomes zero for ideal 2D objects with zero thickness. However, CD of bilayers is mainly a consequence of interlayer electronic coupling, which will rise much more rapidly with decreasing interlayer distance[22]. As the thickness is negligible compared with the wavelength and practically a finite constant for a given material, CD in twisted bilayers can be regarded as a 'chiral effect in the 2D limit'. By contrast, in conventional Kramers–Weyl semimetals, the chiral charge explicitly depends on the continuous band dispersion in the third dimension, so the physics cannot be directly regarded as '2D chiral' even if the material is vdW and can be thinned down to the single-molecular limit.

An apparent trade-off is that a vanishing mechanical coupling between the layers, while making their manipulation easier, will prevent strong chiral physical phenomena distinct from two isolated monolayers. The mechanical coupling strength, measured by the exfoliation energy compared with the formation energy, or the spring constants of interlayer phonons compared with that of in-plane phonons, is generally below 10^{-2} for common vdW materials[40,41]. Therefore, chirality is not expected to have a prominent impact on structural dynamics in twisted 2D materials. Meanwhile, the interlayer electronic hopping can be as large as 10^{-1} of the intralayer hopping in vdW metals and semimetals[42,43]. The ratio may be further boosted in twisted 2D flat-band systems, including moiré superlattices and kagomé lattices, where the effective in-plane hopping diminishes[44,45], and the electronic wavefunction of the twisted flat bands may incur large asymmetry to enable low-energy chiral physics. Similarly, the interlayer magnetic exchange interactions can exceed 10^{-1} of the intralayer exchange in some 2D magnets[46]. When the interlayer exchange also surpasses the single-ion anisotropy, one can expect unusual non-collinear and chiral spin structures in twisted bilayer magnets[34,35]. In addition, hydrostatic pressure and post-assembly intercalation are known to greatly enhance interlayer coupling and potentially amplify chiral effects[47,48]. Thus, many opportunities are envisioned to realize chiral electronic and magnetic states in twisted vdW 2D materials with sufficient interlayer coupling, which have not been thoroughly probed experimentally.

For chiral nanotubes and helices based on 2D ribbons (Fig. 1b), the microscopic chiral effects are caused by the bond deformation. The elastic limit of such deformation is usually on the order of 10^{-1} (ref. 49), smaller than the maximum interlayer twisting in Fig. 1d. But because the intralayer hopping is larger than interlayer hopping, one would expect the magnitude of chiral properties in chiral nanotubes, originating from the twisted intralayer electronic hopping, to be comparable to that from the interlayer hopping in twisted vdW layers. There are notable

https://doi.org/10.1038/s41563-024-01814-2

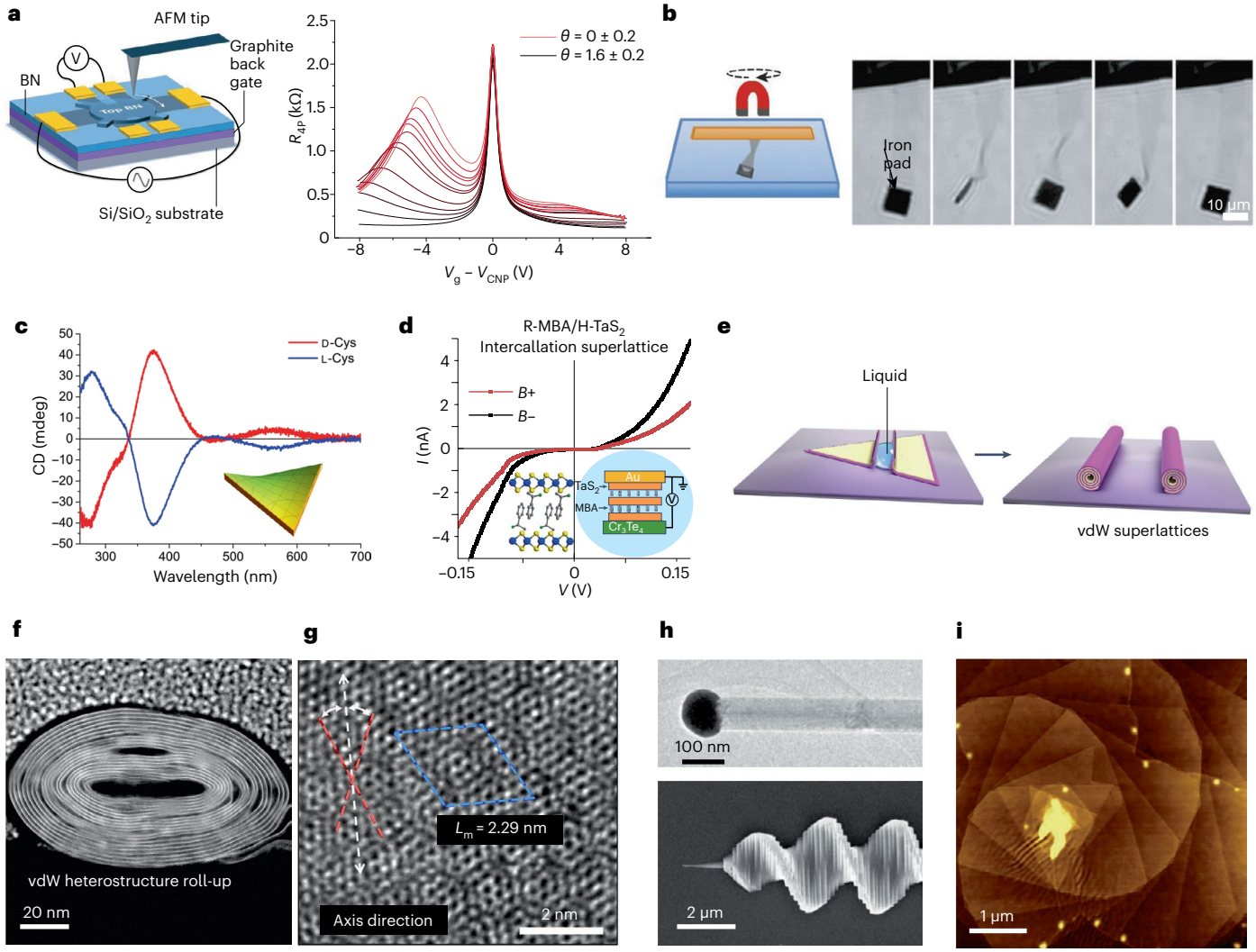

Fig. 3 | Constructing chiral vdW systems using top-down manipulation and bottom-up synthesis. a, Left: tuning the moiré superlattice in graphene by AFM tip-controlled boron nitride (BN) rotor. Right: changing the twisting angle θ and the periodicity of the superlattice shifts the carrier density and gate voltage V_g to reach the secondary Dirac point. V_{CNP}, charge-neutral point; R_{4P}, four-terminal resistance. **b**, A free-standing monolayer graphene in liquid with one end attached to an iron pad, which twists and untwists the graphene under external rotating magnetic fields. **c**, Liquid-exfoliated MoS_2 flakes functionalized by the chiral ligand cystine exhibit CD above the bandgap of MoS_2 but below the onset of the CD spectrum of cystine itself, indicating electronic hybridization between the two materials. Inset: a hypothetical chiral geometry of the functionalized flakes. **d**, H-TaS_2 thin crystal intercalated by R-α-methylbenzylamine (R-MBA) shows a large CISS effect for spins injected from ferromagnetic Cr_3Te_4. The spin polarization is controlled by the external magnetic fields $B\pm$. Insets: the molecular (left) and device (right) structure. **e**, Schematic of surface tension-assisted rolling of vdW superlattices. **f**, Transmission electron microscope image of such a nanoscroll. **g**, Periodic moiré supercell (blue dashed line) formed by the twisted lattice orientations (red dashed line) of the top and bottom walls of the nanoscroll. L_m, moiré superlattice constant. **h**, A GeS nanowire with a screw dislocation grown from a gold nanoparticle (top), whose Eshelby twist is visualized by subsequent lateral extension (bottom). **i**, AFM image of a twisted spiral of WS_2, whose growth is seeded by a WO_x nanoparticle with a radius below 100 nm. Panels adapted with permission from: **a**, ref. 53, AAAS; **b**, ref. 61, Springer Nature Ltd; **c**, ref. 66, American Chemical Society; **d**, ref. 37, Springer Nature Ltd; **e**–**g**, ref. 70, Springer Nature Ltd; **h**, ref. 75, Springer Nature Ltd; **i**, ref. 78. AAAS.

exceptions, though, due to the difference in periodic boundary conditions. For example, chiral carbon nanotubes are mostly semiconductors showing giant resonant optical CD in the visible to near-infrared frequencies[50], in contrast to semimetallic twisted graphene with largest CD in the ultraviolet or mid- to far-infrared frequencies[22,24]. Antiferromagnetic nanotubes with an odd number of unit cells in circumference are expected to be spin frustrated, potentially resulting in non-trivial magnetic states even when the apparent structural chirality is weak[51].

Creating chirality of 2D materials

Twisted vdW stackings may naturally occur at the surface of cleaved vdW crystals or as the stacking faults in as-grown thin films. But to accurately control the twisting angle and chirality, twisted stackings are usually made by tedious manual exfoliation and mechanical alignment. Once the structures are fabricated, the chirality is typically difficult to manipulate, except that it can diminish after the interface undergoes structural relaxation[52]. A powerful technique towards more systematic investigation of 2D chiral phenomena is to mechanically rotate the two layers in vdW contact by atomic force microscope (AFM) tips[53], as shown in Fig. 3a. Both sides of the rotors can be large monolayers made rigid enough against the applied shear force, that is, clamped onto thick solid substrates[54]. The substrates are typically electrically insulating or optically transparent materials to facilitate the measurement of bilayer properties. Meanwhile, even if the rotors are bulk vdW materials, it is still possible that the interfacial chiral properties stand out in electrical transport or optical emission[55].

Apart from twisted stackings, another form of tunable chirality that can be applied to 2D materials is kirigami—the art of creating stable 3D structures from patterned 2D sheets[56]. Chiral kirigami from macroscopic or nanoscale thin films, cut and then buckled under internal or external stress, have shown giant optical activity in a broad wavelength range[57,58]. The design strategy of chiral kirigami is well established, miniaturizable to atom-thin 2D materials, and can achieve chiral bond deformation above 10^{-2}. Such mechanical bending is limited by the strength of the material, which, for 2D materials with open boundaries, is often lower than the elastic limit[59]. Another challenge is to stabilize free-standing and compressed structures against spontaneous vdW adhesion, whose energy is on the order of 0.1 J m^{-2} and comparable to the bending energy for any samples larger than a few square nanometres[60]. Increasing the layer number n of the 2D layers boosts their bending stiffness by n^3 but also reduces the maximum curvature by $1/n$. Surprisingly, monolayers may self-reinforce by thermal fluctuations or static ripples in surfactant solutions, with a bending stiffness more than three orders of magnitude larger than expected, and therefore can be reversibly folded or twisted[61] (Fig. 3b). Tetherless autonomous origamis have also been demonstrated by attaching the monolayers to films as thin as a few nanometres, the deformation being limited by fracture or delamination[62]. The ultimate solution to eliminate such restraints would be patterned Janus monolayers[63], which potentially enable chiral kirigami with bending radius as small as 3 nm, plus strong, field-tunable asymmetric properties[64].

Besides the top-down fabrication approach, chiral 2D materials can be created 'bottom up'. Many techniques developed for assembling supramolecular chiral structures can be adapted to 2D materials[65]. For example, the adsorption of chiral molecules on 2D layers in solutions creates stronger optical activity than that of the molecules themselves. Large CD occurs for photon energies lower than the molecular transition but above the 2D layers' bandgap, indicating electronic hybridization between the molecules and the 2D materials[66] (Fig. 3c). Chirality transfer-induced CD is also demonstrated in quasi-2D hybrid organic–inorganic perovskites incorporating chiral organic cations[67]. As there is no apparent twist in sample geometry or crystalline structure, again it is more likely that the chirality is introduced to the electronic wavefunctions. More generally, chiral molecules can directly intercalate into vdW semimetals without ionic bonding by immersion in pure molecular liquids at a relatively modest temperature[37]. In this work, the CD features of intercalated TaS_2 flakes indicate weak electronic hybridization with the molecules, probably due to the large energy misalignment between the molecular orbitals and the Fermi surface. Nevertheless, the coupling is sufficient to result in strong CISS, where the alignment of the spin orientation and the current direction determines the conductivity (Fig. 3d).

Another bottom-up approach to create geometric chirality is by rolling the 2D sheet into nearly 1D tubules. It is well known that chiral carbon nanotubes have asymmetric optical properties that are distinct from achiral ones, such as relaxed selection rules and large second-harmonic generation, while the flattened graphene nanoribbons have none[68]. Driven by capillary forces, both mono- and heterolayer 2D materials can curl into nanoscrolls and high-order superlattices[69,70], as shown in Fig. 3e,f. The structural chirality is evident from the twist between the top surface and the bottom surface (Fig. 3g), albeit the twisting angle is not precisely controlled. Naively, as the rolling starts from the edge of the flakes, it might be possible to define edges with arbitrary orientation with respect to the crystalline axis through nanolithography, and control the folding angle potentially in a scalable manner for a wafer-size 2D single crystal[71]. Although chiral nanoscrolls have not yet demonstrated asymmetric scattering properties as theory suggested[72], chirality was already found to enhance second-harmonic generation above the optical nonlinearity of the initial 2D sheets[73,74].

Finally, direct growth of vdW layered crystals such as GeS is commonly guided by screw dislocations of Burgers vector b, normal to the layers, and yields chiral structures. Moreover, in a phenomenon called Eshelby twist, the subsequent crystal layers are slightly sheared/rotated, to balance the torque of stress from the dislocation[75,76] (Fig. 3h). Thus, the layers are twisted with an angle inversely proportional to the cross-section S of the crystal at the early stage of growth. The interlayer angle, for a nucleation site of a few nanometres, reaches ~$b^2/S \approx 10^{-2}$ only, as b is about the size of the unit cell dictated by elastic energy penalty. Interestingly, such penalty is absent for hollow thin-wall nanotubes, permitting various b values and posing the challenge of single-chirality growth[77]. The screw dislocation can also be initiated by non-Euclidean surfaces such as nanoparticles, with continuously tunable twist up to 10^{-1} depending on the curvature of the surface[78] (Fig. 3i). At the moment, both methods are non-deterministic, but once a spiral is nucleated, it can keep growing laterally while the twist stays up to wafer size, unrestrained by internal stress from the weak interlayer coupling, which is a unique advantage over 3D crystals. In the future, it may be possible to employ highly monodisperse nanoparticles as nucleation centres to grow flakes with more uniform twisting angles. Overall, both the top-down fabrication and bottom-up synthesis suggest systematic and scalable ways to engineer chiral nearly 2D materials, and should motivate more experiments to discover and quantify chiral properties in such materials.

Future directions of chiral functionalities and manipulation

At present, merely a handful of 2D vdW compounds have been made chiral with the approaches discussed above, leaving vast unexplored territories to enhance and control giant chiral scattering and transport for optoelectronic, spintronic and quantum devices[79]. For instance, the robustness of Kramers–Weyl nodes of chiral materials in the 2D limit has not been investigated, despite recent theory and experiment on 2D Weyl fermions[80,81]. Chiral stackings of 2D vdW magnetic materials grown from curved surfaces potentially enable topological spin textures, unidirectional magneto-plasmons, non-reciprocal magneto-resistance and magnetoelectricity[82]. In non-magnetic chiral 2D materials, similar effects might arise from TRS-breaking 'chiral' electromagnetic environments or phonon excitations[83–85]. 'Truly chiral' electromagnetic fields, which cannot convert to their mirror images by translation/rotation plus time reversal, may be focused by chiral 2D materials to deep subwavelength scale in the near field, and thus may couple stronger to enantioselective photochemistry[86]. It is also possible to observe spin chirality without structural chirality. For instance, spontaneous spin chirality was observed in frustrated 2D lattices and in 2D ferromagnets under external magnetic fields to introduce chiral optical or electronic properties[87,88]. Another potential mechanism to reversibly manipulate chirality is static electric fields, which differentiates stacking types of bilayers by their electric dipole moments[89,90]. Such chiral memories, if proved reproducible on a large scale, can serve as integrated light and spin valves. Compared with 3D bulk chiral materials, one advantage of 2D chiral materials is the electrostatically tunable Fermi surface, which leads to widely adjustable particle–hole symmetry, carrier and spin density, and optical resonance. Besides, 2D systems on proper substrates can dissipate heat more efficiently, and thus potentially endure control fields with higher strength to reach a larger parameter space. Therefore, we believe that chiral nearly 2D vdW materials, beyond the pure geometric charisma, have great potential for both fundamental science and information technology.

References

1. Gasser, J. & Leutwyler, H. Chiral perturbation theory to one loop. *Ann. Phys.* **158**, 142–210 (1984).
2. Qi, X.-L. & Zhang, S.-C. Topological insulators and superconductors. *Rev. Mod. Phys.* **83**, 1057–1110 (2011).

3. Castro Neto, A. H., Guinea, F., Peres, N. M. R., Novoselov, K. S. & Geim, A. K. The electronic properties of graphene. *Rev. Mod. Phys.* **81**, 109–162 (2009).
4. Hsieh, D., Basov, D. N. & Averitt, R. D. Towards properties on demand in quantum materials. *Nat. Mater.* **16**, 1077–1088 (2017).
5. Kennes, D. M. et al. Moiré heterostructures as a condensed-matter quantum simulator. *Nat. Phys.* **17**, 155–163 (2021).
6. Biot, J. B. *Recherches expérimentales et mathématiques sur les mouvements des molécules de la lumiere autour de leur centre de gravité* 408 (Firmin Didot, 1814).
7. Turner, M. D. et al. Miniature chiral beamsplitter based on gyroid photonic crystals. *Nat. Photon.* **7**, 801–805 (2013).
8. Verbiest, T. et al. Strong enhancement of nonlinear optical properties through supramolecular chirality. *Science* **282**, 913–915 (1998).
9. Naaman, R., Paltiel, Y. & Waldeck, D. H. Chiral molecules and the electron spin. *Nat. Rev. Chem.* **3**, 250–260 (2019).
10. Chang, G. et al. Topological quantum properties of chiral crystals. *Nat. Mater.* **17**, 978–985 (2018).
11. Dryzun, C. & Avnir, D. On the abundance of chiral crystals. *Chem. Commun.* **48**, 5874–5876 (2012).
12. Fang, Y., Wang, F., Wang, R., Zhai, T. & Huang, F. 2D $NbOI_2$: a chiral semiconductor with highly in-plane anisotropic electrical and optical properties. *Adv. Mater.* **33**, 2101505 (2021).
13. Geim, A. K. & Grigorieva, I. V. Van der Waals heterostructures. *Nature* **499**, 419–425 (2013).
14. Kreyszig, E. *Differential Geometry* (Dover Publications, 1991).
15. Harris, A. B., Kamien, R. D. & Lubensky, T. C. Molecular chirality and chiral parameters. *Rev. Mod. Phys.* **71**, 1745–1757 (1999).
16. Ding, F., Harutyunyan, A. R. & Yakobson, B. I. Dislocation theory of chirality-controlled nanotube growth. *Proc. Natl Acad. Sci. USA* **106**, 2506–2509 (2009).
17. Xu, F., Yu, H., Sadrzadeh, A. & Yakobson, B. I. Riemann surfaces of carbon as graphene nanosolenoids. *Nano Lett.* **16**, 34–39 (2016).
18. Wang, J. et al. Synthesis of a magnetic π-extended carbon nanosolenoid with Riemann surfaces. *Nat. Commun.* **13**, 1239 (2022).
19. Castellanos-Gomez, A. Why all the fuss about 2D semiconductors? *Nat. Photon.* **10**, 202–204 (2016).
20. Li, G. et al. Observation of Van Hove singularities in twisted graphene layers. *Nat. Phys.* **6**, 109–113 (2010).
21. Carr, S. et al. Twistronics: manipulating the electronic properties of two-dimensional layered structures through their twist angle. *Phys. Rev. B* **95**, 075420 (2017).
22. Kim, C.-J. et al. Chiral atomically thin films. *Nat. Nanotechnol.* **11**, 520–524 (2016).
23. Stauber, T. et al. Neutral magic-angle bilayer graphene: condon instability and chiral resonances. *Small Sci.* **3**, 2200080 (2023).
24. Huang, T. et al. Observation of chiral and slow plasmons in twisted bilayer graphene. *Nature* **605**, 63–68 (2022).
25. Cheong, S.-W. SOS: symmetry-operational similarity. *npj Quantum Mater.* **4**, 53 (2019).
26. Margetis, D. & Stauber, T. Theory of plasmonic edge states in chiral bilayer systems. *Phys. Rev. B* **104**, 115422 (2021).
27. Huang, M. et al. Giant nonlinear Hall effect in twisted bilayer WSe_2. *Natl Sci. Rev.* **10**, nwac232 (2022).
28. Duan, J. et al. Giant second-order nonlinear Hall effect in twisted bilayer graphene. *Phys. Rev. Lett.* **129**, 186801 (2022).
29. He, P. et al. Graphene moiré superlattices with giant quantum nonlinearity of chiral Bloch electrons. *Nat. Nanotechnol.* **17**, 378–383 (2022).
30. Huang, M. et al. Intrinsic nonlinear Hall effect and gate-switchable Berry curvature sliding in twisted bilayer graphene. *Phys. Rev. Lett.* **131**, 066301 (2023).
31. Sodemann, I. & Fu, L. Quantum nonlinear Hall effect induced by Berry curvature dipole in time-reversal invariant materials. *Phys. Rev. Lett.* **115**, 216806 (2015).
32. Stauber, T., Low, T. & Gómez-Santos, G. Chiral response of twisted bilayer graphene. *Phys. Rev. Lett.* **120**, 046801 (2018).
33. Stauber, T., González, J. & Gómez-Santos, G. Change of chirality at magic angles of twisted bilayer graphene. *Phys. Rev. B* **102**, 081404 (2020).
34. Hejazi, K., Luo, Z.-X. & Balents, L. Noncollinear phases in moiré magnets. *Proc. Natl Acad. Sci. USA* **117**, 10721–10726 (2020).
35. Akram, M. et al. Moiré skyrmions and chiral magnetic phases in twisted CrX_3 (X = I, Br, and Cl) bilayers. *Nano Lett.* **21**, 6633–6639 (2021).
36. Bahamon, D. A., Gómez-Santos, G. & Stauber, T. Emergent magnetic texture in driven twisted bilayer graphene. *Nanoscale* **12**, 15383–15392 (2020).
37. Qian, Q. et al. Chiral molecular intercalation superlattices. *Nature* **606**, 902–908 (2022).
38. Gatti, G. et al. Radial spin texture of the Weyl fermions in chiral tellurium. *Phys. Rev. Lett.* **125**, 216402 (2020).
39. Young, S. M. & Kane, C. L. Dirac semimetals in two dimensions. *Phys. Rev. Lett.* **115**, 126803 (2015).
40. Mounet, N. et al. Two-dimensional materials from high-throughput computational exfoliation of experimentally known compounds. *Nat. Nanotechnol.* **13**, 246–252 (2018).
41. Zhao, Y. et al. Interlayer breathing and shear modes in few-trilayer MoS_2 and WSe_2. *Nano Lett.* **13**, 1007–1015 (2013).
42. Doran, N. J., Titterington, D. J., Ricco, B. & Wexler, G. A tight binding fit to the bandstructure of 2H-$NbSe_2$ and NbS_2. *J. Phys. C* **11**, 685 (1978).
43. Tong, Q. et al. Topological mosaics in moiré superlattices of van der Waals heterobilayers. *Nat. Phys.* **13**, 356–362 (2017).
44. Leykam, D., Andreanov, A. & Flach, S. Artificial flat band systems: from lattice models to experiments. *Adv. Phys. X* **3**, 1473052 (2018).
45. Balents, L., Dean, C. R., Efetov, D. K. & Young, A. F. Superconductivity and strong correlations in moiré flat bands. *Nat. Phys.* **16**, 725–733 (2020).
46. Li, B. et al. Quasi-two-dimensional ferromagnetism and anisotropic interlayer couplings in the magnetic topological insulator $MnBi_2Te_4$. *Phys. Rev. B* **104**, L220402 (2021).
47. Yankowitz, M. et al. Dynamic band-structure tuning of graphene moiré superlattices with pressure. *Nature* **557**, 404–408 (2018).
48. Lu, Z., Carr, S., Larson, D. T. & Kaxiras, E. Lithium intercalation in MoS_2 bilayers and implications for moire flat bands. *Phys. Rev. B* **102**, 125424 (2020).
49. Sawada, S. & Hamada, N. Energetics of carbon nano-tubes. *Solid State Commun.* **83**, 917–919 (1992).
50. Ghosh, S., Bachilo, S. M. & Weisman, R. B. Advanced sorting of single-walled carbon nanotubes by nonlinear density-gradient ultracentrifugation. *Nat. Nanotechnol.* **5**, 443–450 (2010).
51. Sakai, T., Sato, M., Okamoto, K., Okunishi, K. & Itoi, C. Quantum spin nanotubes—frustration, competing orders and criticalities. *J. Phys. Condens. Matter* **22**, 403201 (2010).
52. Feng, X., Kwon, S., Park, J. Y. & Salmeron, M. Superlubric sliding of graphene nanoflakes on graphene. *ACS Nano* **7**, 1718–1724 (2013).
53. Ribeiro-Palau, R. et al. Twistable electronics with dynamically rotatable heterostructures. *Science* **361**, 690–693 (2018).
54. Hu, C. et al. In-situ twistable bilayer graphene. *Sci. Rep.* **12**, 204 (2022).
55. Lee, H. Y. et al. Tunable optical properties of thin films controlled by the interface twist angle. *Nano Lett.* **21**, 2832–2839 (2021).
56. Zhang, Z., Tian, Z., Mei, Y. & Di, Z. Shaping and structuring 2D materials via kirigami and origami. *Mater. Sci. Eng. R* **145**, 100621 (2021).

57. Liu, Z. et al. Nano-kirigami with giant optical chirality. *Sci. Adv.* **4**, eaat4436 (2018).
58. Choi, W. J. et al. Terahertz circular dichroism spectroscopy of biomaterials enabled by kirigami polarization modulators. *Nat. Mater.* **18**, 820–826 (2019).
59. Yang, Y. et al. Intrinsic toughening and stable crack propagation in hexagonal boron nitride. *Nature* **594**, 57–61 (2021).
60. Koenig, S. P., Boddeti, N. G., Dunn, M. L. & Bunch, J. S. Ultrastrong adhesion of graphene membranes. *Nat. Nanotechnol.* **6**, 543–546 (2011).
61. Blees, M. K. et al. Graphene kirigami. *Nature* **524**, 204–207 (2015).
62. Miskin, M. Z. et al. Graphene-based bimorphs for micron-sized, autonomous origami machines. *Proc. Natl Acad. Sci.* **115**, 466–470 (2018).
63. Lu, A.-Y. et al. Janus monolayers of transition metal dichalcogenides. *Nat. Nanotechnol.* **12**, 744–749 (2017).
64. Berry, J., Ristić, S., Zhou, S., Park, J. & Srolovitz, D. J. The MoSeS dynamic omnigami paradigm for smart shape and composition programmable 2D materials. *Nat. Commun.* **10**, 5210 (2019).
65. Liu, M., Zhang, L. & Wang, T. Supramolecular chirality in self-assembled systems. *Chem. Rev.* **115**, 7304–7397 (2015).
66. Purcell-Milton, F. et al. Induction of chirality in two-dimensional nanomaterials: chiral 2D MoS_2 nanostructures. *ACS Nano* **12**, 954–964 (2018).
67. Long, G. et al. Spin control in reduced-dimensional chiral perovskites. *Nat. Photon.* **12**, 528–533 (2018).
68. Barros, E. B. et al. Review on the symmetry-related properties of carbon nanotubes. *Phys. Rep.* **431**, 261–302 (2006).
69. Xie, X. et al. Controlled fabrication of high-quality carbon nanoscrolls from monolayer graphene. *Nano Lett.* **9**, 2565–2570 (2009).
70. Zhao, B. et al. High-order superlattices by rolling up van der Waals heterostructures. *Nature* **591**, 385–390 (2021).
71. Liao, M. et al. Precise control of the interlayer twist angle in large scale MoS_2 homostructures. *Nat. Commun.* **11**, 2153 (2020).
72. Tepliakov, N. V. et al. Chiral optical properties of tapered semiconductor nanoscrolls. *ACS Nano* **11**, 7508–7515 (2017).
73. Qian, Q. et al. Chirality-dependent second harmonic generation of MoS_2 nanoscroll with enhanced efficiency. *ACS Nano* **14**, 13333–13342 (2020).
74. Xia, H. et al. Probing the chiral domains and excitonic states in individual WS_2 tubes by second-harmonic generation. *Nano Lett.* **21**, 4937–4943 (2021).
75. Liu, Y. et al. Helical van der Waals crystals with discretized Eshelby twist. *Nature* **570**, 358–362 (2019).
76. Sutter, P., Wimer, S. & Sutter, E. Chiral twisted van der Waals nanowires. *Nature* **570**, 354–357 (2019).
77. Yakobson, B. I. & Bets, K. V. Single-chirality nanotube synthesis by guided evolutionary selection. *Sci. Adv.* **8**, eadd4627 (2022).
78. Zhao, Y. et al. Supertwisted spirals of layered materials enabled by growth on non-Euclidean surfaces. *Science* **370**, 442–445 (2020).
79. Aiello, C. D. et al. A chirality-based quantum leap. *ACS Nano* **16**, 4989–5035 (2022).
80. Mella, J. D. & Torres, L. E. F. F. Robustness of spin-polarized edge states in a two-dimensional topological semimetal without inversion symmetry. *Phys. Rev. B* **105**, 075403 (2022).
81. Lu, Q. et al. Observation of 2D Weyl fermion states in epitaxial bismuthene. Preprint at https://arxiv.org/abs/2303.02971 (2023).
82. Cheong, S.-W. & Xu, X. Magnetic chirality. *npj Quantum Mater.* **7**, 40 (2022).
83. Hübener, H. et al. Engineering quantum materials with chiral optical cavities. *Nat. Mater.* **20**, 438–442 (2021).
84. Zhu, H. et al. Observation of chiral phonons. *Science* **359**, 579–582 (2018).
85. Luo, J. et al. Large effective magnetic fields from chiral phonons in rare-earth halides. *Science* **382**, 698–702 (2023).
86. Stauber, T., Low, T. & Gómez-Santos, G. Plasmon-enhanced near-field chirality in twisted van der waals heterostructures. *Nano Lett.* **20**, 8711–8718 (2020).
87. Grohol, D. et al. Spin chirality on a two-dimensional frustrated lattice. *Nat. Mater.* **4**, 323–328 (2005).
88. Ding, B. et al. Observation of magnetic skyrmion bubbles in a van der Waals ferromagnet Fe_3GeTe_2. *Nano Lett.* **20**, 868–873 (2020).
89. Stern, M. V. et al. Interfacial ferroelectricity by van der Waals sliding. *Science* **372**, 1462–1466 (2021).
90. Weston, A. et al. Interfacial ferroelectricity in marginally twisted 2D semiconductors. *Nat. Nanotechnol.* **17**, 390–395 (2022).

Acknowledgements

H.Z. acknowledges grants from the National Science Foundation (DMR-2240106) and the Welch Foundation (C-2128). B.I.Y. acknowledges the Office of Naval Research grants N00014-22-1-2788 and N00014-22-1-2753, and the Kavli Exploration Award in Nanoscience.

Competing interests

The authors declare no competing interests.

Additional information

Correspondence should be addressed to Zhu or Yakobson.

Peer review information *Nature Materials* thanks Tobias Stauber and the other, anonymous, reviewer(s) for their contribution to the peer review of this work.